Dual Stage Passive Vibration Isolation for Optical Interferometer Missions

Allen J. Bronowicki [*a], Rhonda MacDonald [a], Yekta Gursel [b], Renaud Goullioud [b], Timothy Neville [b] and David Platus [c]
[a] TRW Space & Electronics Group; [b] Jet Propulsion Laboratory; [c] Minus-K Technology Inc.

ABSTRACT

Future space-based optical instruments such as the Space Interferometer Mission have vibration-induced error allocations at the levels of a few nano-meters and milli-arc-seconds. A dual stage passive isolation approach has been proposed using isolation first at the vibration-inducing reaction wheels, and a second isolation layer between the bus portion of the space vehicle (the backpack) and the optical payload. The development of the backpack isolator is described, with unit transmissibility results for individual isolator struts.

The dual stage isolation approach is demonstrated on a dynamically feature-rich, 7-meter structural testbed (STB3). A new passive suspension that mitigates ground vibrations above 0.4 Hz has been integrated into the testbed. A series of OPD performance predictions have been made using measured transfer functions. These indicate that the 5-nm dynamic OPD allocation is within reach using the dual isolator approach. Demonstrating these low response levels in a noisy air environment has proven to be difficult. We are sequentially executing a plan to mitigate acoustic transmission between backpack and flight structure, as well as developing techniques to mitigate effects of background acoustic noise.

Key words: vibration isolation, jitter, pathlength control

1. INTRODUCTION

The Space Interferometry Mission (SIM) flight vehicle will be a surveying instrument of unprecedented precision. It will allow the measurement of stellar positions to a relative accuracy of micro-arc-seconds [1]. This accuracy will be achieved over a baseline of ten meters between the light collecting siderostat mirrors. This requires measuring distances to the target star to accuracies on the order of 50 pico-meters. The mirrors need not be positioned that well, as the SIM external metrology system measures their relative positions. However, there are dynamic stability constraints in order for the science and metrology interferometers to function at this accuracy. To preserve fringe stability, 10 nm of relative dynamic motion between the arms of the science interferometer has been allocated as an allowable [2]. Of that motion, 5 nm has been sub-allocated for dynamic response of the spacecraft to spacecraft-induced disturbances [3].

1.1 SIM Structural Dynamic Design

The structural design of the SIM flight vehicle is described in Reference 3. The Precision Structure Subsystem (PSS) is a monolithic (non-deployable), low-distortion graphite/polycyanate structure. It holds the instrument optics in two collector pods at the plus and minus Y ends, and in a combiner bay in the middle, as shown in Figure 1. Its first bending mode frequency approaches 25 Hz in the current design. All of the spacecraft equipment, as well as the majority of instrument electronics, is housed in a "backpack" structure. The backpack need not be dimensionally stable, and hence is constructed from aluminum due to its low cost and good thermal conductivity. Low frequency appendages such as the solar array and communications antenna are attached to the backpack.

The only vibration disturbances on the PSS are dithering mechanisms within the metrology system. The motion of these devices is miniscule, and at rates below those likely to excite structural dynamics of the flight vehicle. The primary vibration sources on SIM are the six reaction wheels in the backpack. SIM employs two layers of passive vibration isolation to mitigate this. The first layer is a hexapod isolator mount for each reaction wheel. This design is identical to the one operating on the Chandra X-ray Observatory [4,5], operating in the vicinity of 10 Hz. The second isolation layer is a set of three beams disposed between the backpack and PSS. The beams are flexured in such a way that they transmit only bending loads, with stiffness and damping set near 5 Hz and 4%, respectively. The backpack

[*] allen.bronowicki@trw.com; (310) 813-9124, fax: -4686; One Space Park Drive, R4/1120,Redondo Beach, CA, USA 90278

isolator is intended to be as soft as possible while still supporting the weight of the backpack, allowing ground testing without a separate gravity offload system. Using the dual isolator approach, simulations predict that the dynamic stability requirement will be met with margin with two of the six reaction wheels dwelling simultaneously at the worst wheel speed.

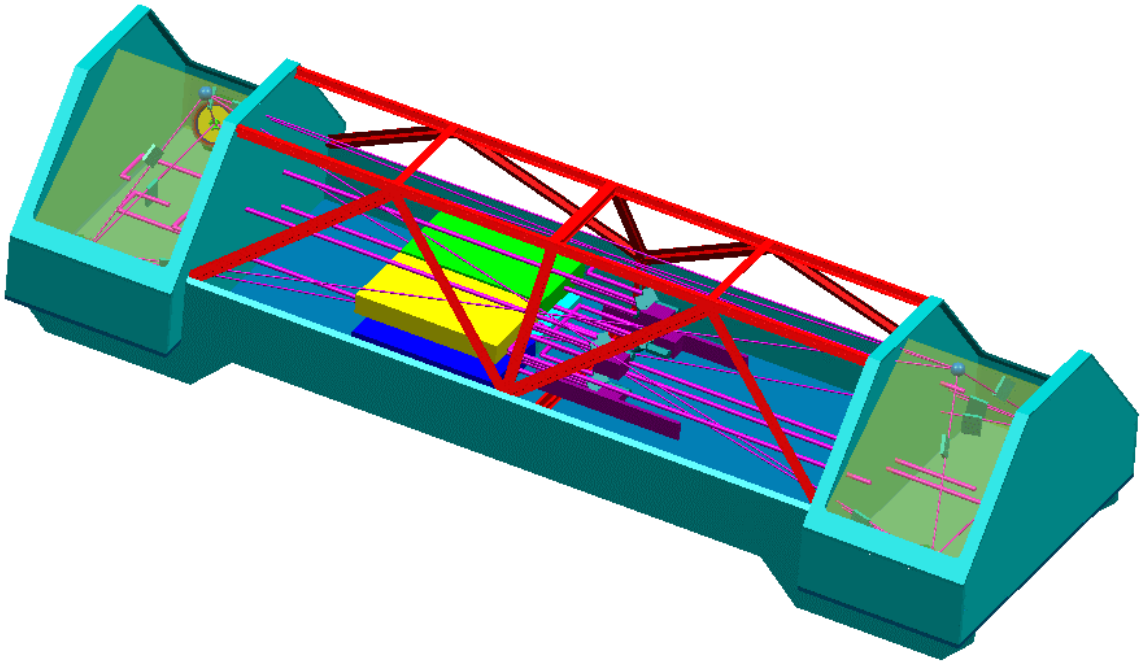

Figure 1. Cutaway View of SIM Reference Design Precision Structure

1.2 System Test Bed for Verification of SIM Dynamics and Control.

The SIM System Test Bed 3 (STB3) is being built and exercised to verify that the vibration isolation and active optics systems will work together to achieve the dynamic stability goals. Work to date on active optics development [6] has taken place on an isolated optical bench, not on a structure scaled dynamically to behave similarly to the flight SIM. The active optics hardware is slated to be moved onto the STB3 flexible structure in FY 2003 to test the effects of control-structure interaction. This paper describes the work to date on STB3 structural dynamics. The only optics currently on the structure is a laser metrology system [7] that measures baseline distance between the "science" siderostat pallets.

2. THE STB3 STRUCTURE AND SUSPENSION

The STB3 structure and suspension is shown in Figure 2. The structure consists of both precision structure and backpack simulators. The backpack can be locked to the PSS or suspended on the vibration isolator whose natural frequency is 5 Hz in vertical bounce.

2.1 Precision Structure Subsystem

The dimensions of the STB3 PSS are 9m long by 1.5m wide by 0.5m deep. It is constructed from aluminum panels with 0.93" thick honeycomb core and 20 mil aluminum facesheets. These panels are bonded together using Π–shaped aluminum extrusions. The panels have numerous cutouts to mitigate vibro-acoustic interactions. Three optical pallets, that will eventually hold the collecting optics for the science and two guide interferometers, are mounted at each end of the PSS. The extreme +Y (West) and –Y (East) pallets currently have posts holding retro-reflectors for the baseline measuring laser interferometer, as well as X and Y accelerometers for dynamic optical path difference measurements (pseudo-OPD). There are two mass-simulated pallets in the middle of the PSS. These locations will eventually hold the science and guide interferometer combiner optics. One pallet holds a Y-accelerometer for pseudo-OPD.

The fundamental modes of the PSS with backpack isolated is Z-bending at 10.4 Hz, torsion near 16 Hz, and X-bending near 25 Hz. There is a pair of beam-combiner sway modes between 12 and 13 Hz. Beyond these, there are numerous vibration modes involving elaborate combinations of outrigger, beam combiner, siderostat pallet and PSS deformation, making this a very dynamically rich structure. The STB3 PSS stiffness was intended to emulate that of the flight system, which at that time was a folding structure designed for launch on an expendable launch vehicle, with a deployed first mode of 12 Hz. The flight PSS design has since evolved into a monolithic structure that will fit into the Space Shuttle cargo bay. Much greater depth is now available, resulting in a first bending mode greater than 20 Hz.

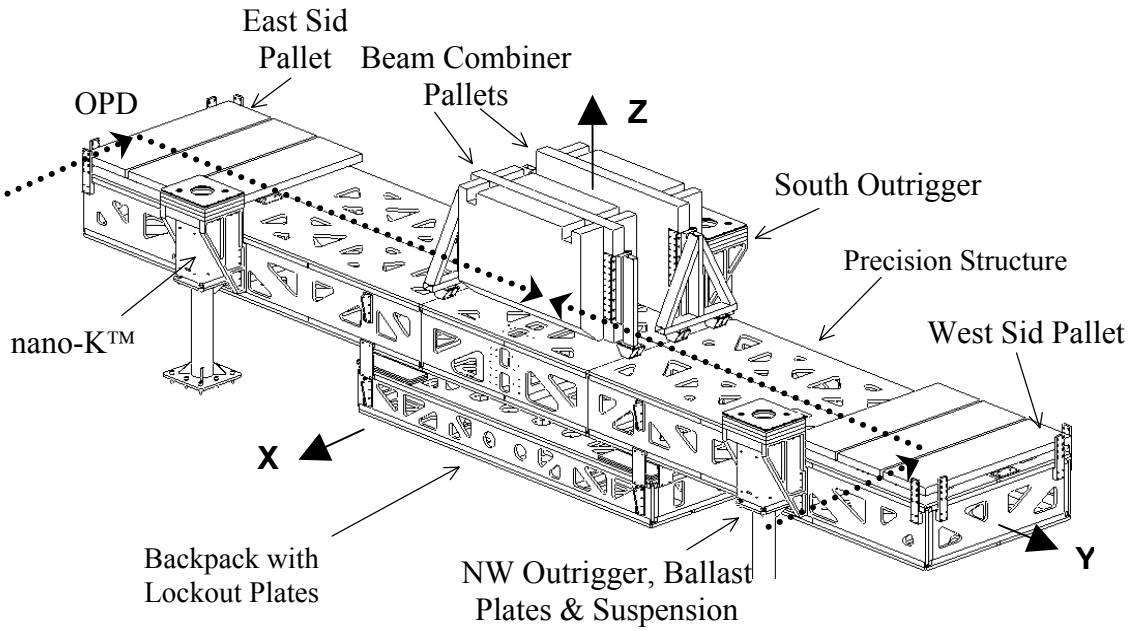

Figure 2. STB3 Structure and Suspension

2.2 Backpack

The backpack dimensions are 3.1m long by 1.5m wide by 0.36m deep. Its construction is similar to that of the PSS. The backpack has ballast at each of four corners, bringing its total mass up to 240 kg. A plate to which the shaker and reaction wheel isolator can be mounted is located in the southwest corner. The fundamental backpack modes are torsion at 46.8 Hz and Z-bending at 66.3 Hz. These are similar to those of the flight backpack. A CAD drawing of the backpack and isolator struts is shown in Figure 3. The six plates used occasionally to lock out the isolator for the hardmount condition are also shown.

2.2 Backpack Isolator

The isolator consists of three struts cantilevered from a stiff region in the center of the backpack, connecting through A-flexures to hard points on the PSS. Each strut is a laminated tubular construction. An inner tube built from fiberglass carries the static load of the backpack. The inner tube is over-wrapped with a layer of viscoelastic material (VEM). The VEM in turn is covered with a graphite constraining layer that is segmented at intervals along its length. This increases the transfer of load from the inner tube to the outer tube through the VEM, enhancing damping [8, 9]. The three struts and mounting components are shown in Figure 4 prior to installation.

2.3.1 Strength Analysis and Test

The greatest concern in the design of the isolator was static strength in the isolator beams under earthquake load from the backpack. Using 1.5G design acceleration, and dividing the vertical load into bending on each of three struts results in a lateral design limit load of 265 pounds. This produces a root stress of 15,700 psi, a corresponding axial strain of 0.39%, and predicted tip sag of 0.62 inches. For these parameters, the predicted failure mode is slight cracking in the epoxy of

the off-angle fiberglass. The ultimate strength had been predicted to be in the neighborhood of 400 pounds. To confirm the design load, a test to destruction was planned on a prototype strut.

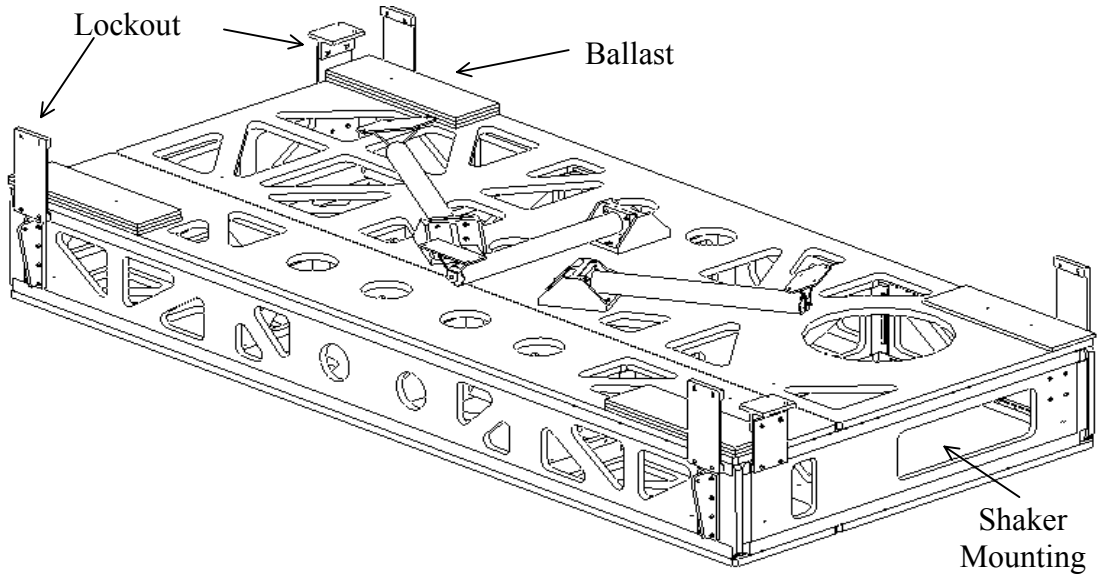

Figure 3. STB3 Backpack and Isolator Struts

In fact, 1,000 pounds of lateral load was applied to the strut with no noticeable damage. This is almost four times the design load. The strut tip deflected 2.85" laterally, a considerable distortion across such a short beam. Peak root strain would have had to have been on the order of 1.7% to produce this deflection. Thus, it was demonstrated that the static capability of the isolator struts is significantly greater than allowed by standard composite design practice, which predicts failure for minute cracking in the matrix of any ply, off-axis plies in this case.

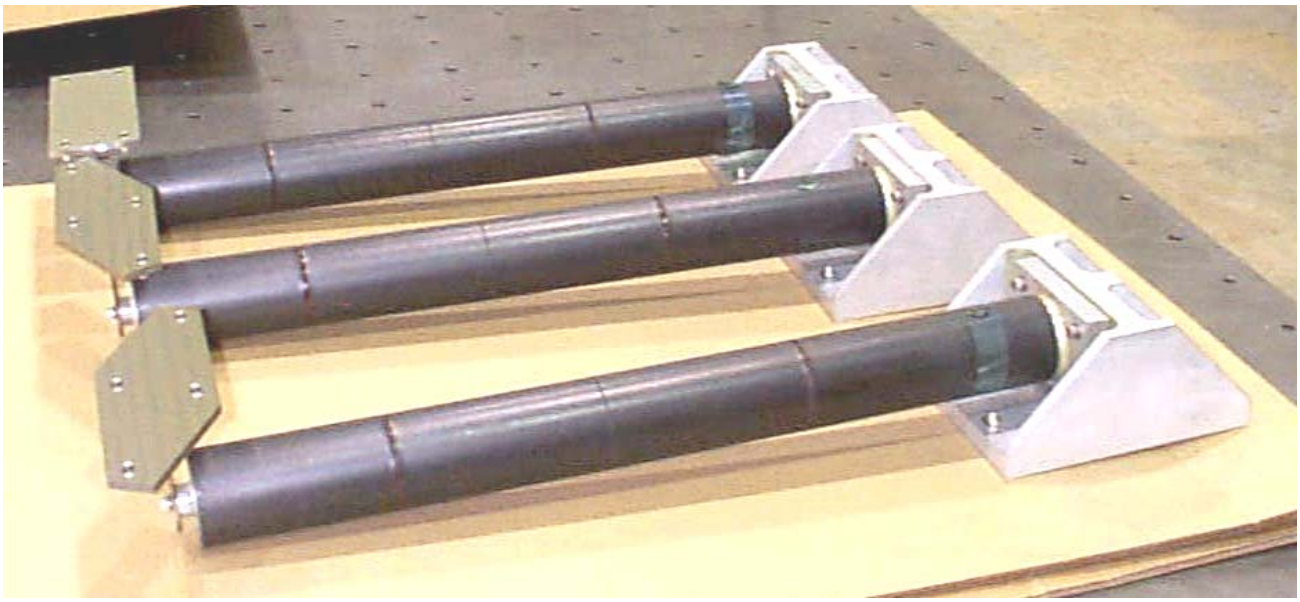

Figure 4. Backpack Isolator Struts Prior to Installation

2.3.2 Unit Strut Transmissibility Tests

Each isolator strut was subjected to a unit level test to confirm stiffness, damping and lateral vibration transmissibility. Three deliverable struts, along with the proof-loaded prototype were tested. The tests were conducted with the base of each strut fixed, and a tip mass of 67 kg, somewhat less than one third of the entire backpack mass. Comparative analysis was performed using a model incorporating the frequency and temperature dependent properties of the VEM. The first mode, primarily involving lateral translation of the tip mass, was predicted to be 5.4 Hz with damping of 4.4%. Tests revealed the actual frequency to be 5.6 Hz with damping of 3.4%. The second mode, involving local bending within the strut with the tip almost pinned, was predicted to be 514 Hz, with damping of 5.6%. Tests showed frequency of 464 Hz with 3.0% damping. The repeatability between all four struts was remarkable, as can be seen in Figure 5. This is evidence that the prototype strut survived the "test to destruction" unscathed. The measurements also compare well with the finite element model prediction.

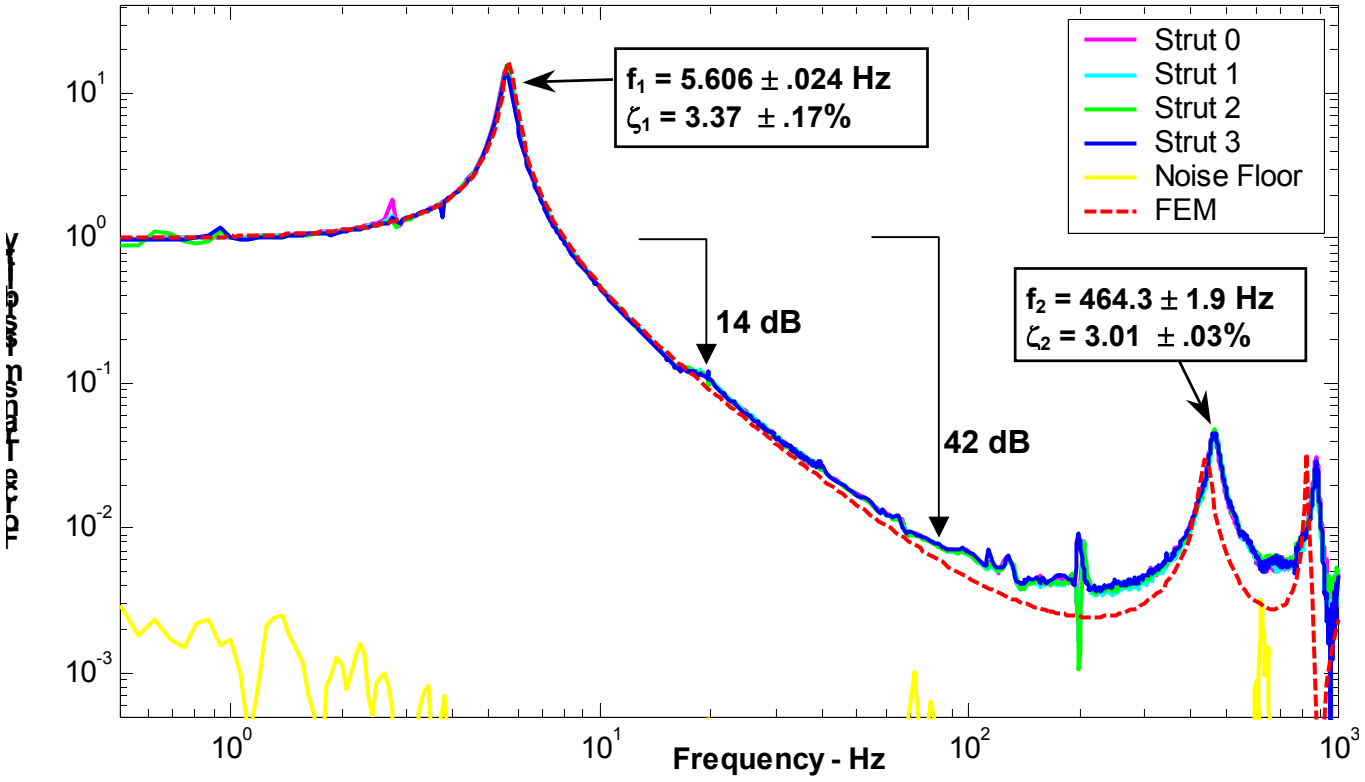

Figure 5. Unit Isolator Strut Force Transmissibility. Repeatability between Four Struts. Comparison to Model.

Lateral force transmissibility is found from shear load measured at the base of the strut, divided by lateral force applied to the tip mass. In the reaction wheel speed range of 15 to 80 revolutions per second (rps), vibration attenuation was found to vary from 14 dB to 42 dB. Dynamics in the frequency region above 80 Hz can only be excited by higher harmonics of the wheel disturbance, which have a lower magnitude than the fundamental imbalance forces. In this high frequency region, attenuation is no worse than 26 dB. Vibration attenuation at the low end of the wheel speed range could be made stronger with a lower frequency isolator. This is not currently required due to interoperability with the active optics. Active pathlength control is planned to reject disturbances with a bandwidth of f_0=100 Hz. Below f_0 the attenuation function is approximated analytically by $A(f) = (f/f_0)^{1.5}$. Thus at the lowest wheel speed, 15 rps, active optics will contribute an additional 24 dB of attenuation, bringing the total from isolator and active optics to 38 dB. In

the next phase of STB3, planned for FY 2003, the active optics will be installed on the structure. Fully compensated motions can then be measured, to determine whether 5 nm of pathlength stability can actually be achieved.

2.3.3 Backpack Isolator Modes

The fixed-pinned lateral stiffness of an individual isolator strut is $K_S=3E_{dynamic}I/L^3$. Due to the viscoelastic material's frequency dependence, the dynamic stiffness at the operating frequency of the isolator is employed. For an STB3 strut, the lateral dynamic stiffness at 5 Hz is 456 pounds/inch. For the entire backpack, vertical and lateral stiffnesses are $K_Z=3\ K_S$ and $K_X=K_Y=1.5\ K_S$, respectively. The backpack isolator is thus stiffer in the vertical direction, as all three struts are active, and less stiff laterally due to axial load release in the A-flexures. From a strength viewpoint, this is advantageous, since it allows support of a larger load, while maintaining an even softer suspension laterally.

Transfer function testing has shown frequencies of the backpack isolator modes to be as follows: pitch about Y=2.7 Hz, yaw about Z=3.0, roll about X=3.1, sway in Y=4.65, sway in X=5.0 and bounce in Z=5.2 Hz. The bounce and sway frequencies are somewhat greater than one would expect for the backpack isolator fixed to a solid mount. This is because the PSS is almost free on the negative stiffness suspension. Thus, this is a two-body problem, with neither PSS nor backpack being completely restrained

2.3 Negative Stiffness Mechanism Suspension

The STB3 suspension utilizes nano-K™ mechanical vibration isolators manufactured by Minus-K Technology [10]. Three isolators are placed beneath outriggers from the structure, as shown in Figure 6. The outriggers are disposed slightly above and symmetrically around the structure's mass center in a horizontal plane to ensure stability. The system natural frequency is 0.4 Hz, vertical and horizontal. The isolators are designed for a maximum weight load of approximately 667 kg and a maximum STB3 structure weight of approximately 2000 kg. The initial STB3 structure weight is less than this and ballast has been applied to each outrigger to allow for weight growth.

The nano-K™ isolators utilize negative stiffness mechanisms to negate the stiffness of conventional support springs, producing the low vertical stiffness. An optical-mechanical servo system maintains vertical position within a +/- 0.010-inch deadband by adjusting the force on a small control spring. Optical sensors indicate when the position is outside the deadband and a gear motor automatically adjusts the force on the control spring. The servo system is designed to handle small load changes, temperature changes and long term creep of the support springs. Either a manual load adjustment feature or a change in ballast weight can be used to bring the isolator into the range of the servo system. Once the system is centered, the servo system can be turned off. If there is no weight change and no large temperature change, the suspension remains stable for a relatively long time. Several days of stability is typical on STB3.

The low horizontal stiffness is provided by a set of beam-columns loaded by the weight load to approach their critical buckling load. The 0.4 Hz frequency is achieved over a relatively small weight range that establishes the upper weight limit for the isolator.

Figure 6. nano-K™ Suspension Element on Post, with Outrigger from PSS. .

3. FULL-STRUCTURE TRANSMISSIBILITY TESTS

Transmissibility measurements were conducted for the full STB3 structure in order to determine if the stability goals are being met. Transfer functions (TFs) are measured between force applied to the backpack and either baseline distance or OPD. These TFs are taken for excitations in the X, Y and Z directions. Moments were not measured since the reaction wheel moment excitation is a minor contributor to response. The transfer functions are convolved with an analytic

reaction wheel disturbance model [11] for wheels spinning about X, Y and Z. This produces a quasi-measured OPD spectrum versus wheel speed. One can view this spectrum either as-computed (raw) or after the application of the active optics disturbance rejection function.

3.1 Test Configuration and Instrumentation

Tests were conducted in the following configurations: Hardmount, with backpack locked to PSS and wheel mass simulator bolted to backpack; Backpack Isolated, with wheel still locked; and Dual Stage, with both isolators active.

For the wheel hardmount cases, the mass simulator is bolted to the floor of the backpack. For the isolated wheel case, the simulator was mounted on three NewDamp™ elastomeric isolators. The shaker-wheel isolator combination is shown mounted on a breadboard in Figure 7. The frequencies of the "wheel isolator" were measured as 18 Hz lateral and 21 Hz vertical, with very heavy damping. These are twice as high as the isolation frequencies of the flight isolator, so vibrations in the wheel speed range are not well attenuated. The wheel isolator does attenuate high frequency vibration considerably, and alleviates sound radiation from the backpack, by limiting backpack panel response. Installation of a softer first isolation stage is planned for FY 2003.

A non-contact actuator was used to excite the backpack. The device employs a coil with cooling fins attached to a 120-lb steel mass on elastomeric isolators. This base isolation mitigates the propagation of high frequency reaction forces into the floor. The coil drives a Nd-Fe-B magnet. The force imparted to the magnet is measured using a quartz load cell monitored by a high gain charge amplifier. The actuator delivers 4.65 Newton/Amp, and the load cell sensitivity is 146 Newton/Volt. The magnet is mounted to the "reaction wheel". The optical path difference (OPD) to a hypothetical star can be computed using a combination of inertial vibration measurements. 10 Volt/G accelerometers with a further amplifier gain of 10 are used for this purpose. Signals from X and Y accelerometers on the extreme East and West siderostats, as well as a Y accelerometer on the North combiner pallet are combined (see Figure 2). The sum is divided by frequency-squared to convert to displacement. The pseudo-OPD measurement is OPD = $-X_{West} + Y_{West} + X_{Eest} + Y_{East} - 2\,Y_{Comb}$. The East and West siderostat pallets also have posts holding retro-reflectors for the baseline measuring laser interferometer [6]. The sensitivity of the gauge is $\lambda/2/\#$ fractional counts. Since wavelength is λ =1,319 nm, and the phase-meter has 640 counts per half wavelength, there is 1.03 nm per count. The interferometer is sampled at 200 KBPS, 32 samples are averaged and then sent to a digital-to-analog converter for re-sampling by the data acquisition system. The sensitivity of the DAC is 844 nm/Volt. The averaging process enhances resolution by the square root of number of averages, giving an effective resolution of 0.2 nm. In the future, a larger dynamic range will be obtained by leaving the data in a digital form. The baseline measurement is simply BL = Y_{West}-Y_{East}. This can also be measured in a pseudo fashion using accelerometers collocated on the retro posts, one of which is shown in Figure 8.

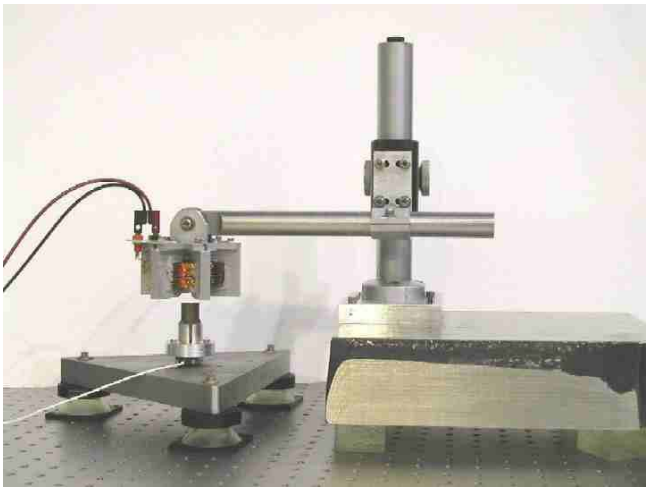

Fig. 7. Reaction wheel Mass Simulator on NewDamp Isolators plus Non-Contact Actuator on Isolated Block.

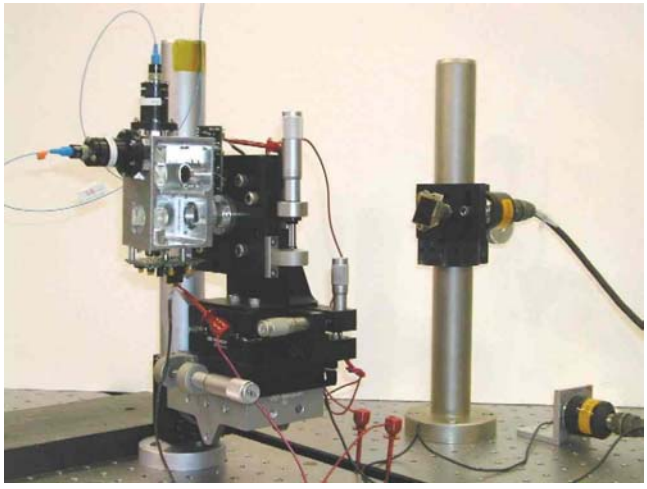

Figure 8. Beam Launcher and West Sid Retro with X and Y Accelerometers

3.2 Vibro-acoustic Concerns

At one point the backpack was completely disconnected from the PSS and supported on foam blocks sitting on the floor. Transmissibility was measured, revealing that vibrations above 100 Hz were being transmitted from backpack to PSS without any mechanical path (except possibly through the foam, floor and suspension). Acoustic transmission from the backpack panels to PSS panels was deemed to be the culprit. With the wheel hardmounted, backpack panel vibrations are easily felt with one's fingers. The TFs above 200 Hz, isolated backpack or backpack on floor, were quite similar, indicating that acoustics was the dominant form of vibration transmission. To block the acoustic sneak path around the backpack isolator, an acoustic barrier enclosure was built around the entire backpack, with small holes for the isolator strut A-flexures. The barrier was constructed from ¾" plywood, with a double layer of ¼" acoustic foam and 0.1" dense limp vinyl barrier material, about 1.5" of barrier in all. The barrier fits in a 2.5" gap between the top of the isolator struts and the bottom of the PSS. In addition, barrier material was added to the panel to which the wheel simulator was mounted; 1.5" sound absorbing foam was placed beneath the entire backpack, and sound absorbing foam wedges were placed at one end. Finally, the shaker reaction mass was isolated from the floor as described above. The net effect of this vibro-acoustic mitigation was a reduction in vibration transmission above 200 Hz: by a factor of 3 to 10 for the hardmount backpack case; and by a factor of 1 to 10 in the isolated backpack case. Below 200 Hz the effect of the vibro-acoustic mitigation was difficult to ascertain.

3.3 Transfer Function Results

Transfer function measurements were taken in three frequency bands: 0-50 Hz with 25 averages; 45-245 Hz with 50 averages; and 200-1000 Hz with 100 averages. A typical set of transfer function measurements for pseudo-OPD is shown in Figure 9 for a vertical, Z-axis excitation. In the hardmount case there is considerable resonant activity between 10 and 100 Hz. The backpack isolator alone mitigates this considerably. In fact, the suppression of response below 100 Hz is near that of an ideal isolator. Also evident in the isolated backpack TF are the well-damped isolation modes at 3 and 5 Hz. Above 100 Hz, it is likely that acoustic transmission starts to predominate, so that only a small benefit is seen from the backpack isolator.

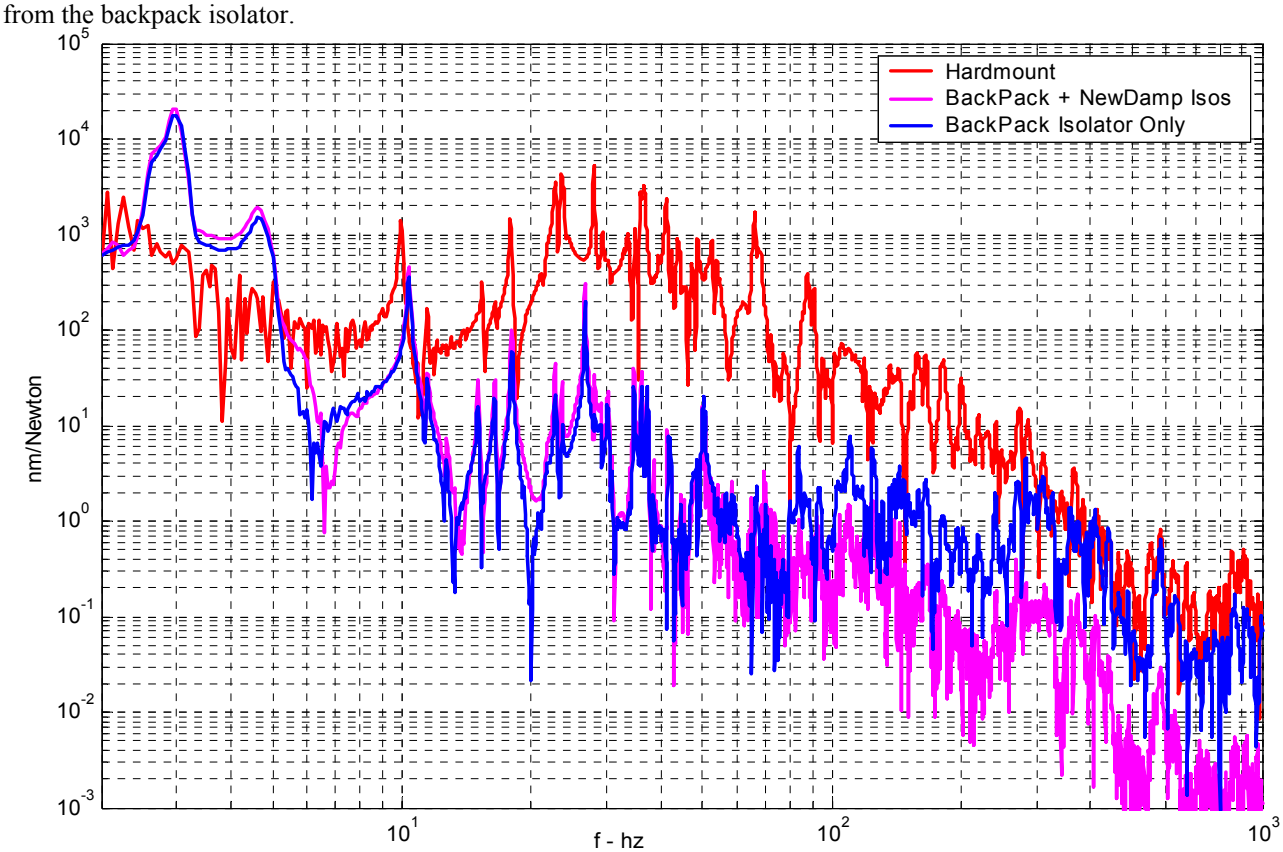

Figure 9. Pseudo-OPD Transfer Functions for Excitation in Z.

In the dual stage case, the approximately 20 Hz "wheel" isolator amplifies vibrations between 10 and 40 Hz. A significant benefit is seen above 100 Hz. Together, the dual-stage isolation system makes the high frequency vibrations inconsequential. Better isolation may be demonstrated if further progress is made at blocking acoustic propagation of vibration, or were tests to be conducted in vacuum.

The accuracy of the baseline measurement with the laser gauge is displayed in Figures 11 and 12. The measurements were taken with the backpack isolated and the wheel locked, for a Z-excitation.

Figure 10 contrasts transfer functions using optical baseline measurement with pseudo-baseline using accelerometers. From 5 to 300 Hz the correspondence is remarkable. This indicates that both measurements are very accurate. Below 5 Hz the accelerometer becomes susceptible to drift, being a piezo-electric device, which must maintain charge to maintain signal. Above 300 Hz there are some differences in the two measurements. It could be that modes of the post introduce phase shifts between the laser retro and the accelerometer. The laser hits its noise floor above 300 Hz. The accelerometer has better sensitivity than the laser at high frequency, and resolves features in the tens of pico-meters. This discrepancy in noise floor was even more evident in the dual isolator configuration due to very low signals at high frequency. That is why the backpack isolator case is presented.

Figure 11 shows the Fourier spectrum of the laser gauge for this test. Features as small as 100 pico-meters are resolved. The high resolution is achieved by averaging in the laser gauge, as well as in the data acquisition system. An RMS signal of 1,500 nano-meters was measured, so that a dynamic range greater than 80 dB has been achieved in the laser gauge.

3.4 Convolved OPD Predictions

The bottom line on performance is the computed optical path difference using measured transfer function data. The disturbance rejection of the active optics is folded in analytically. Figure 12 shows the predicted OPD based on accelerometer data for the three cases considered

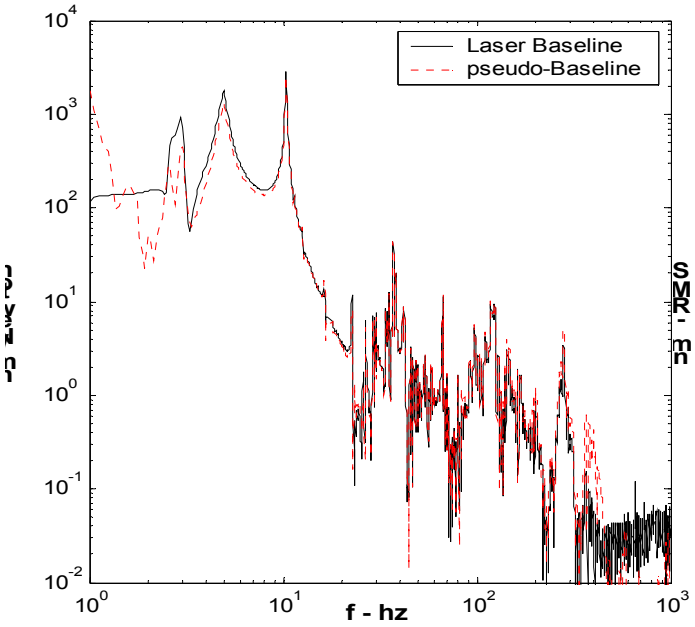

Figure 10. Comparison Between Laser and Pseudo Baseline Transfer Function Measurements

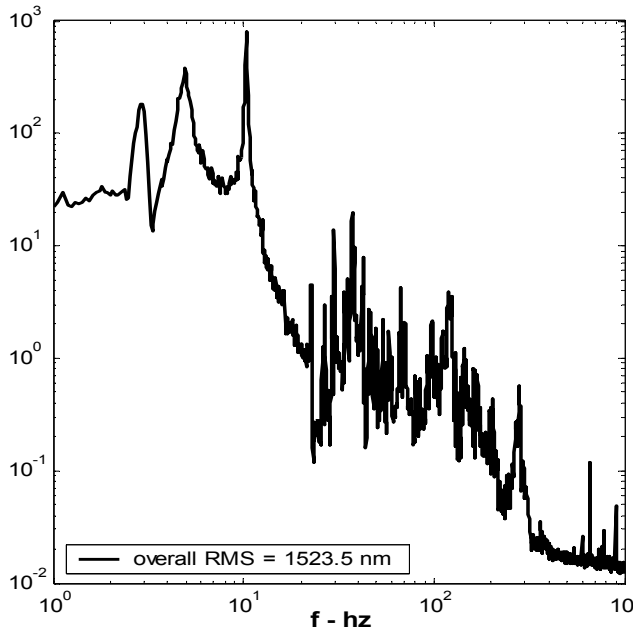

Figure 11. Laser Baseline Fourier Spectrum

In the hardmount case vibrations are very deleterious, with OPD predicted to be as high as 1,600 nm. This vastly exceeds the allocation of 5 nm for response to spacecraft disturbances. The single backpack isolator brings vibration down to 15 nm, a two order of magnitude reduction. The second isolator stage actually makes vibration worse below 50 revolutions per second (rps), but improves matters above that wheel speed. Above 52 rps the dual isolator achieves the goal, with OPDs no greater than 3 nm. Thus at the higher wheel speeds a three order of magnitude reduction is

achieved. The next step in STB3 development, installation of a more compliant isolator at the "wheel", should permit us to meet the fringe visibility error budget over a much greater range of wheel speeds.

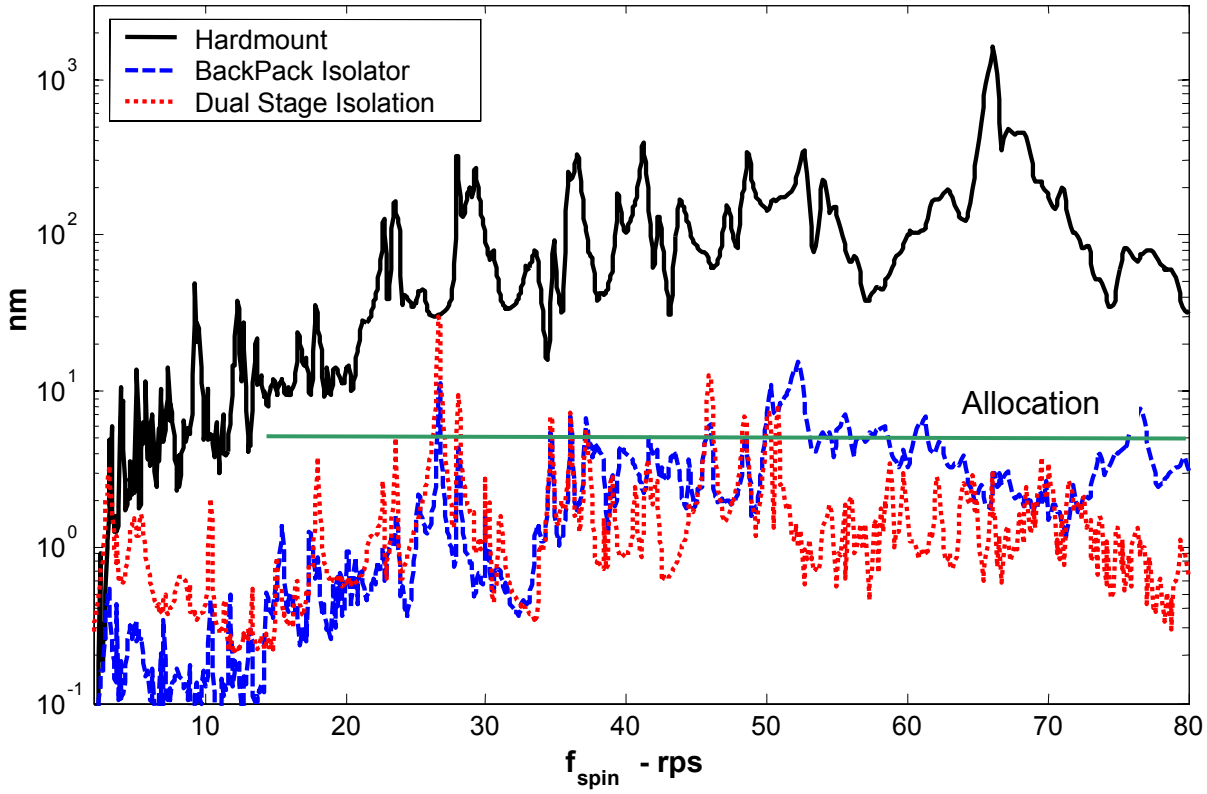

Figure 12. OPD Prediction Based on Measured Accelerometer Data, after Analytic Active Optics Attenuation.

4. CONCLUSIONS

SIM's System Test Bed 3 is evolving into a capability for resolving numerous dynamics and control issues. To date, it has demonstrated the effectiveness of the dual stage isolation approach at mitigating high frequency reaction wheel vibrations, which have been pushed down almost to the sensor noise floor. In the mid-range of frequencies, from 10 to 50 Hz, another factor of approximately 5 rejection is still required. This can be accomplished by lowering the frequency of the first isolator stage, as is currently planned. An increased understanding of dynamics in the precision structure may allow some of the response to be mitigated through the addition of structural damping. The usefulness of STB3 is in allowing these complex trades to be explored on the ground prior to committing to a flight design.

Our experience has also pointed out the difficulties of trying to demonstrate sub-nano-meter performance in an air environment. Notice that sensor resolution in the pico-meter range is required for the transfer function approach we are using. Further challenges lie in learning how to deal with acoustic transmission paths and background acoustic noise.

ACKNOWLEDGMENTS

The research described in this publication was carried out at TRW and at the Jet Propulsion Laboratory, California Institute of Technology, under a contract with the National Aeronautics and Space Administration. The results presented are the fruits of effort by many people. We particularly thank John Innis for building and setting up much of the instrumentation and John Shaw for his work in numerous hardware setups.

REFERENCES

1. Danner, R. and Unwin, S., editors, "Space Interferometry Mission, Taking the Measure of the Universe", *JPL 400-811,* 1999.
2. SIM Science Requirements Document, 1999.
3. Brady, D. H., et al, "Structural Design Challenges for a Shuttle-launched Space Interferometry Mission," *Proc. SPIE*, *Vol. 4852-60*, Interferometry in Space, August, 2002.
4. Nye, T. W., Bronowicki, A. J., Manning, R. A., and Simonian, S. S., "Applications of Robust Damping Treatments to Advanced Spacecraft Structures," *Guidance, Navigation & Control Conf.,* Breckenridge CO, 1997.
5. Pendergast, K. J., Schauwecker, C. J., "Use Of A Passive Reaction Wheel Jitter Isolation System To Meet The Advanced X-Ray Astrophysics Facility Imaging Performance Requirements," *Proc. SPIE, Vol. 3356*, Space Telescopes and Instruments V, pp. 1078-1094, 1998
6. Goullioud, R., Alvarez Salazar, O. S., "Dim Star Fringe Stabilization on the SIM Testbed 3 using Pathlength Feed-forward of the "Guide" Interferometer Optical Path," *Proc. SPIE*, Vol. 4852-52, *Interferometry in Space*, August, 2002.
7. Goullioud R., Azizi A., "Optical design of the SIM System Testbed 3", *Proc. SPIE*, vol. 4006, *Interferometry in Optical Astronomy*, pp. 788-799, 2000.
8. Plunkett, R. & Lee, C. T., "Length Optimization for Constrained Viscoelastic Layer Damping," *J. of Acoustical Society of America*, *Vol. 48, No.1* pp. 150-161, 1970.
9. Bronowicki, A. J. and Diaz, H. P., "Analysis, Optimization, Fabrication and Test of Composite Shells with Embedded Viscoelastic Layers," paper GCA in *Damping '89*, W-P AFB Report WRDC-TR-89-3116.
10. Platus, D. L., "Negative-Stiffness-Mechanism Vibration Isolation Systems," *Proc. SPIE*, Vol. 3786, Optomechanical Engineering and Vibration Control, 1999, pp. 98-105.
11. Masterson, R. A., and Bronowicki, A. J., "Simplified Teldix RDR 68-4 RWA and Isolator Models," *TRW IOC M740-61*, March 31, 2000.